Original Article
Toxicology International, *May-Aug 2016 / Vol-23 / Issue-2, 178-188*
ISSN (Print) : 0971-6580
ISSN (Online) : 0976-5131
DOI: 10.22506/ti/2016/v23/i2/146699

Mouse mesothelium–derived cell lines: models to assess cytotoxic effects of novel nanomaterials *in vitro* and to ultimately investigating carcinogenesis *in vivo*

Sarah Lutz[1], Saskia Perret-Gentil[1], Laszlo Pecze[1], Thomas Henzi[1], Jean-François Dechézelles[2], Beat Schwaller[1] and Walter Blum[1]*

[1]Anatomy, Department of Medicine, University of Fribourg, Route Albert-Gockel 1, 1700 Fribourg, Switzerland
[2]BioNanomaterials Group, AdolpheMerkle Institute, University of Fribourg, Chemin des Verdiers 4, 1700 Fribourg, Switzerland
* walter-vincent.blum@unifr.ch

Abstract

Novel nanomaterials are continuously produced, but still little is known about their potential toxic and carcinogenic effects. In contrast, crocidolite is one of the best-characterized asbestos types known to induce nanotoxicity and to transform mesothelial cells resulting in malignant mesothelioma. Only in few reports mesothelial or mesothelioma-derived cells were used to investigate nanotoxicity and/or carcinogenicity. Even less studies were carried out with mouse-derived cell lines allowing to investigating nanotoxicity *in vivo*. Immortalized mesothelial cells from wildtype (iMeso-WT1), from NF2+/- heterozygous (iMeso-NF3) mice and the NF2+/- mouse-derived mesothelioma cell line RN5 were used to compare acute cytotoxicity between novel silica-based manufactured nanoparticles (MNP) and crocidolite. All cell lines were sensitive to crocidolite-induced cytotoxicity, but rather resistant to the spherical MNP, with iMeso-NF3 being the most sensitive and RN5 being the least sensitive cells. Chronic exposure (1 month) of iMeso-NF3 cells to a sub-lethal dose of crocidolite resulted in increased acute resistance to crocidolite. Yet, asbestos-resistant iMeso-NF3 cells didn't induce tumors after intraperitoneal injection, while RN5 cell injection resulted in macroscopic tumors after 5 weeks. Thus, mouse mesothelium-derived cell lines appear well suited to study potential hazardous health effects of MNP.

Keywords: *In vitro* mesothelium model, NF2, mesothelial cells, asbestos, RN5, silica particles

Received: 10-05-2016 **Revised:** 30-06-2016 **Accepted:** 08-07-2016

1. Introduction

Manufacturing and designing novel nanoparticles are occurring at an extremely rapid pace and virtually daily novel nanoparticles and nanofibers are brought to the market. The particular properties of manufactured nanoparticles (MNP) make them suitable for diverse applications ranging from aerospace industry to biomedicine bearing an overwhelming diversity and functionalization potential (Dechézelles et al., 2013; Stark et al., 2015). It is essential to assess potential health hazards of MNP (Donaldson and Poland, 2012). The mesothelium, a monolayer of mesothelial cells covering internal organs of the pleural, peritoneal and pericardial cavities (Mutsaers, 2004) is considered to be a most sensitive structure, particularly susceptible towards one type of fiber-based structures, i.e. naturally occurring asbestos fibers (Bocchetta et al., 2000).Thus, mesothelial cells maintained *in vitro* represent a useful model to investigate not only asbestos fiber toxicity, but also to investigate MNP toxicity. Since primary mesothelial cells (prMC) have a limited life span(Blum et al., 2015a) and

* *Author for correspondence*

cell maintenance *in vitro* requires numerous additional supplements in the growth medium (Pecze and Schwaller, 2015) we have previously generated immortalized mouse mesothelial cell lines, either from wildtype (WT) mice (iMeso-WT1) or from mice heterozygous for the tumor suppressor NF2 (iMeso-NF3), both on a C57Bl/6J background as well as a mouse mesothelioma cell line RN5 (Blum et al., 2015b). Cells with decreased NF2 levels are of high relevance, since the *NF2* gene is mutated in 40% of all human malignant mesothelioma (Felley-Bosco and Stahel, 2014; Thurneysen et al., 2009). RN5 cells were previously shown to be tumorigenic *in vivo* after subcutaneous xenografting, while iMeso-WT1 and iMeso-NF3 cells, both SV40-immortalized mesothelial cell lines are non-tumorigenic (Blum et al., 2015b). Here we aimed to investigate the potential of murine immortalized mesothelial cells (iMeso) and RN5 mesothelioma cells to serve as models to assessing acute MNP nanotoxicity and to compare it to the known asbestos-induced acute cytotoxic effects. We also investigated whether immortalized mesothelial cells might serve as a model to follow the transformation process, i.e. to determine the carcinogenic potential of nanomaterials, either *in vitro* or *in vivo*.

2. Materials and Methods

Tetraethyl orthosilicate (TEOS), 3-(aminopropyl) triethoxysilane (APTES, 99%) and rhodamineisothiocyanate (RITC, mixed isomers) were supplied by Sigma-Aldrich (Buchs,Switzerland). Absolute ethanol (Reagent ACS) was obtained from Honeywell International Inc. (Rolle, Switzerland). Ammonium hydroxide aqueous solution (25 %) was purchased from Sigma-Aldrich (Buchs, Switzerland). 2-[methoxy(polyethyleneoxy)propyl]trimethoxysilane was obtained from ABCR (Karlsruhe, Germany). Dialysis tubular membrane (MWCO exclusion limit at 14,000 Da, from Carl Roth GmbH, Arlesheim, Switzerland) was used for purification. All aqueous solutions were prepared with ultrapure water obtained from a Milli-Q system (18.2 MΩ·cm, Millipore AG, Schaffhausen, Switzerland).

2.1 Fluorescent Coupling Agent Synthesis

The rhodamine-labeled silica particles were synthesized in a two-step process. The first step consisted in the coupling of RITC with APTES to allow for covalently attaching the dye to the silica network during particle formation. RITC was coupled to APTES via an addition reaction of the amino (-NH_2) group of APTES onto the isothiocyanate (-NCS) group of RITC according to the protocol described by Verhaegh *et al.* (Verhaegh and Blaaderen, 1994). In a glass flask, RITC (100 mg) was dissolved in ethanol. After solubilization, 150 mL of APTES were added and the reaction was kept going for 24 h with stirring in the dark, the latter to prevent photobleaching of the dye.

2.2 100 nm fluorescent silica particles synthesis (Nano31 and 34)

Fluorescent silica particles were synthesized according to a modified Stöber-Fink-Bohn method in the presence of the fluorescent coupling agent. Milli-Q water (13.5 mL), 7.8 mL of ammonia solution(25 %) and 208 mL of ethanol were introduced in a round bottom flask equipped with a refrigerating system. The mixture was thermo-stabilized at 55°C and stirred at 400 rpm. Once the temperature was stabilized, 22 mL TEOS were added. Three minutes later, 600 µL of fluorescent coupling agent was introduced and the reaction solution was stirred for 24 h. The particle suspension was then dialyzed against Milli-Q water.

2.3 1140-nm fluorescent silica particles synthesis (Nano30 and 35)

100 mL of ethanol and 20 mL of ammonia solution (25 %) were introduced in a round flask and stirred at 400 rpm. In parallel, an ethanol-containing solution of TEOS (1.5:3.5;v:v) was prepared and added drop-wise by the means of an infusive pump at a rate of 8 mL/h. After the addition of 2 mL of this mixture, 150 µL of fluorescent coupling agent were added in the syringe and the mixture was added again, still at 8 mL/h. The particle suspension was then dialyzed against Milli-Q water.

2.4 240-nm silica particles synthesis (Nano90)

Milli-Q water (36 mL), 24 mL of ammonia solution (25 %) and 180 mL of ethanol were introduced in a round bottom flask equipped with a refrigerating system. The mixture was thermo-stabilized at 60°C and stirred at 400 rpm. Once a stable temperature of 60°C was reached, 11 mL TEOS was added and the reaction was maintained with stirring for 24 h. The particle suspension was dialyzed against Milli-Q water.

2.5 PEG functionalization (for Nano34 and 35)

Fluorescent silica particles were functionalized with PEG by following a procedure modified from Graf *et al.* (Graf et al., 2012). A silica particle suspension (15 mL; concentration: 38 g/L for 100-nm particles and 60 g/L for 1140-nm particles) was mixed with 75 mL of absolute ethanol in a flask under stirring. Then, 1 mL of PEG-silane was added, followed by 6 mL of ammonia (25 %) solution. The reaction mixture was heated to 80°C and kept under stirring for 12 hours. The particle suspension was then dialyzed against absolute ethanol or centrifuged/re-dispersed in ethanol.

2.6 Characterization of newly synthetized nanomaterials

TEM experiments were performed on a Philips CM100 Biotwin microscope as used previously in other studies (Szabolcsi and Celio, 2015), operated at 80 kV and equipped with a side mounted MORADA CCD camera and a FEI Tecnai Spirit, operated at 120 kV and equipped with a Valeta CCD camera (Olympus), with an image resolution of 2048 times 2048 pixels. One drop of the particle suspensions diluted in absolute ethanol (1:10) was deposited on a 200mesh carbon membrane-coated copper grid and the ethanol slowly evaporated.

2.7 Dynamic light scattering experiments

Dynamic light scattering (DLS) experiments were carried out using a light scattering goniometer instrument (3D LS Spectrometer, LS Instruments, Fribourg, Switzerland) equipped with a HeNe laser light source with a wavelength $\lambda = 632.8$ nm. The samples were filled into cylindrical glass tubes and placed in the temperature-controlled index-matching bath. Measurements were performed at 90°C.

2.8 Cell culture

Two immortalized mouse mesothelialcell lines derived from mice with a C57BL/6J genetic background were used: iMeso-WT1 from a WT mouse and iMeso-NF3 from a NF2+/- mouse as described before (Blum et al., 2015b). The tumorigenic mouse mesothelioma cell line RN5 had been established before from a NF2+/- mouse injected with asbestos fibers (Blum et al., 2015b). All cells were cultured in DMEM-GlutaMax (Gibco, Basel, Switzerland) and supplemented with 10% heat-inactivated fetal bovine serum (FBS;Gibco) and antibiotics (10,000 U/mL penicillin, 10 µg/mL streptomycin (Gibco)). Cells were maintained in a humidified atmosphere at 37°C containing 5% CO_2.

2.9 Cytotoxicity assays and cell proliferation curves

For the determination of cell viability and cell proliferation 125 cells per well of a 96-well plate were seeded and experiments were carried out as described before (Henzi et al., 2009). Briefly, after an overnight incubation, 100 µl of fresh DMEM containing different amounts of nanomaterials were plated to obtain different nanomaterial densities in the various wells (0, 0.5, 1, 2, 4, 7, 14 and 28 µg/cm^2). The MTT (3-(4,5-dimethylthiazol-2-yl)-2,5-diphenyltetrazolium bromide) assay that reports the combined effects of proliferation (number of viable cells) and cellular metabolic activity (Mosmann, 1983) was performed after 140h of nanomaterial exposure as described before (Blum and Schwaller, 2013). Briefly, 10 µl of MTT (1 mg/ml) was added to every well (including control wells containing MNP and medium, but no cells) and plates were incubated for 3 h at 37°C. Then, the medium was removed and formazan crystals were dissolved with 200 µl DMSO (dimethyl sulfoxide) by orbital shaking for 1h. Plates were measured at 570 nm using a Victor X3 spectrophotometer (PerkinElmer). As reported before using the identical method, the solubilization of formazan crystals by DMSO is quantitative and not vulnerable to artifacts caused by the lumping of formazan crystals with MNP alone.Thus, in the absence of cells, the background absorbance is the same in the absence or presence of MNP (Horváth et al., 2011; Magrez et al., 2009). Real-time cell proliferation curves were determined using the Incucyte live-cell imaging system (EssenBioscience, Ann Arbor, MI).

2.10 Chronic crocidolite exposure

iMeso-NF3 cells (180,000) were seeded out in 10-cm diameter petri dishes (TPP, Trasadingen, Switzerland) corresponding to a density of 125 cells in a well of a 96-well plate and exposed one day later to 4 µg/cm^2 NIEHS crocidolite (Brand Crocidolite Bulk Asbestos, SPI Supplies, PA, USA). Cells were passaged weekly (1:10 dilution) and exposed continuously to a density of 4 µg/cm^2 of crocidolite for a period of 28 days. Before injection of treated cells into mice, they were passaged one more time in the absence of crocidolite fibers to remove

extracellular-attached crocidolite fibers. These cells were termed iMeso-NF3-AsbR, the latter part referring to asbestos-resistant.

2.11 Intraperitoneal injection of RN5 cells and iMeso-NF3-AsbR cells

3-4 animals (C57Bl/6J mice, 6-8 week old) per group were injected intraperitoneally (i.p.) with 5 x 10^6 cells that have been resuspended in 500 µl PBS. Mice were palpated daily and sacrificed, when tumors were noticeable, i.e. at day 37 post-injection (for RN5 cells). iMeso-NF3-AsbR injected mice were sacrificed at day 50 post-injection.

2.12 Histological sections

Mice were sacrificed and specimens were collected and fixed for 4 days in 4% paraformaldehyde (PFA) solution and embedded in paraffin as described before (Blum et al., 2015a). Sections (3 µm) were cut and stained by the Goldner staining method.

2.13 Western Blot assay for NF2

Western blot assays were performed essentially as described before (Blum et al., 2015b). Cells were grown in 25 cm^2 cell culture flasks (TPP) until they reached 60-90% confluence. Cells were trypsinized (0.05%), pelleted (500 x g, 3 min), and washed three times with CMF-PBS. Proteins were extracted using RIPA buffer (50 mMTris, 150 mMNaCl, 0.1% SDS, 0.5% sodium deoxycholate, 1% Triton X-100, pH 7.4), incubated for 30 min at 4°C, centrifuged 30 min at 17,000 x g at 4°C and the supernatant was collected. The DC assay (BioRad) was performed in order to quantify the proteins (manufacturer's instructions). Protein samples were separated on a 10% polyacrylamide SDS gel and transferred onto nitrocellulose membranes. Membranes were stained with Ponceau S to check for equal loading. Membranes were blocked with 5% albumin in PBS for 1 h at room temperature and incubated overnight at 4°C with antibodies recognizing NF2 (dilution 1:1,000; Santa Cruz Biotechnology, Heidelberg, Germany, clone A-19). Secondary biotinylated antibodies were applied at a dilution of 1:20,000 and incubated with the ABC system (Vectastain, Vector Laboratories, Burlingame, CA) for 30 min. The HRP substrate (Millipore, Luminata Forte) following the manufacturer's instructions was used on the membranes and the images were collected on a Western blot reader (FluorChem E System, Bucher Biotec, Basel, Switzerland).

2.14 Cell cycle analysis

The Fucci (Fluorescent, ubiquitination-based cell cycle indicators) plasmids CSII-EF-mVenus-hGem and hCdt1-mCherry were a kind gift of Prof. Miyoshi (Riken, Japan) and used as described before (Blum and Schwaller, 2013). Briefly, iMeso-NF3 cells were transfected with the lenti virusmVenus-hGem and hCdt1-mCherry. A clone derived from a single transfected cell was selected, expanded and then exposed for 28 days to 4 µg/cm^2 to crocidolite. This clone was called iMeso-NF3-AsbR-CCI; CCI stands for cell cycle indicator. The duration of the G_0/G_1 phase as well for the $S/G_2/M$ was determined as described before (Blum et al., 2015a).

2.15 Cell death Assay

CellTox Green Cytotoxicity assay (Promega) was performed using the manufacturer's instructions. Briefly, 10,000 cells were seeded in 24-well plates (TPP) and CellTox Green added at a 1:1000 dilution, the mean fluorescence was measured using the IncucyteLiveCell Imaging System for 72h.

3. Statistical Analysis

Each experiment was repeated at least three times ($n \geq 3$) in triplicates and results are presented as mean ± standard deviation. Statistical analysis was performed using an ANOVA with StatPlus.

4. Results

4.1 Cellular nanomaterial toxicity assessment in immortalized mesothelial cell lines iMeso-WT1, iMeso-NF3 and RN5 mesothelioma cells after exposure to crocidolitein vitro

Real-time growth curves in the absence of crocidolite revealed both immortalized mesothelial cells to grow slower than RN5 cells (Fig. 1A). The absence of one functional *Nf2* allele in iMeso-NF3 cells had no statistically significant effect on cell growth. The effect of crocidolite was assessed at 140 h, a time point when all three cell lines had reached near confluence (Fig. 1A). Cells were exposed to a density of crocidolite fibers ranging from 0.5 µg/cm^2 to 28 µg/cm^2 and the effect of crocidolite was determined by the MTT assay measuring

the combined effects of proliferation and cell viability (Fig. 1B). A strong dose-dependent decrease of the MTT signal reflecting cytotoxicity was observed in all three cell lines. Interestingly, iMeso-NF3 cells showed the highest sensitivity towards crocidolite induced-cytotoxicity at all doses tested. Up to 2 µg/cm² iMeso-WT cells were as resistant as RN5 mesothelioma cells, but at higher fiber densities RN5 cells showed clearly the highest resistance towards the cytotoxic effects of crocidolite fibers; some viable and proliferating cells were observed even at the highest concentration (28 µg/cm²).

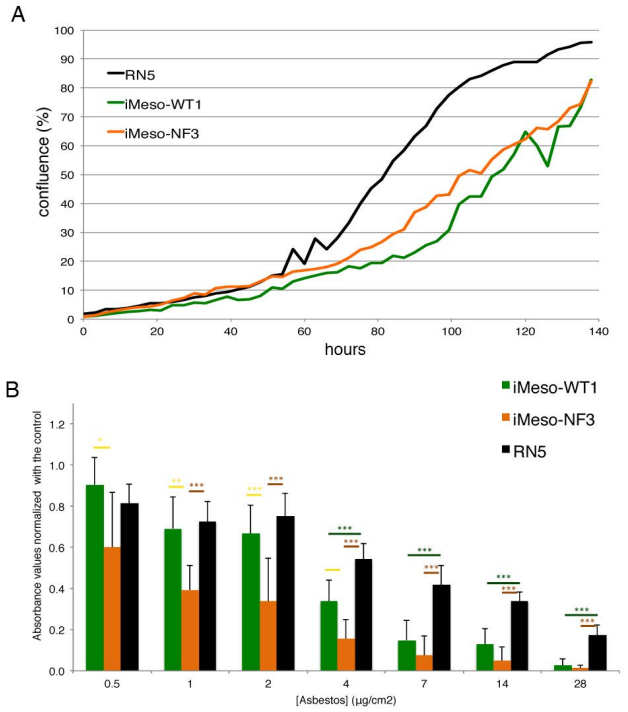
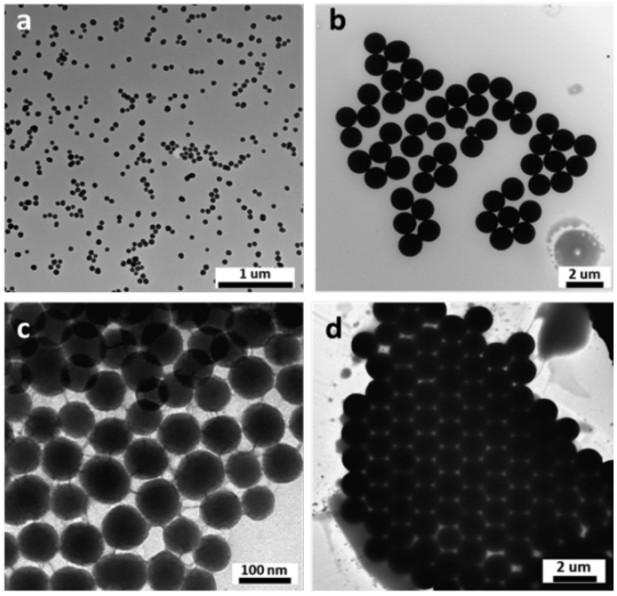


Figure 1. Real-time cell proliferation of mesothelium-derived cell lines and dose-dependent crocidolite-induced cytotoxicity (A) Cell proliferation of cell lines of mesothelial origin monitored for 140h. RN5 mouse mesothelioma cells grew faster than the two immortalized (non-transformed) iMeso cell lines from either WT (iMeso-WT1) or Nf2+/- mice (iMeso-NF3). (B) Effect of crocidolite (doses ranging from 0.5 µg/cm² to 28 µg/cm²) on the viability/growth of the three cell lines exposed to crocidolite for 140h. For the normalization, MTT signals of untreated cells were used and defined as 1.0. Strong concentration-dependent effects on cell proliferation/viability were observed using the MTT assay. The most sensitive cells revealed to be iMeso-NF3 and the most resistant ones to crocidolite exposure were RN5 cells. Few RN5 cells even survived a dose of 28 µg/cm². Lines with asterisk(s) above the bars represent the levels of significance for the respective comparisons. The asterisks indicate the p-values: * = p<0.05, ** = p<0.005 and *** = p<0.0005, N=6 independent experiments.

4.2 Characterization of silica-based nanomaterials

The hydrodynamic diameter of the silica-based nanomaterials was measured by dynamic light scattering and the diameter was additionally measured by transmission electron microscopy (TEM). Both types of measurements gave essentially identical results (Fig. 2); the smaller fluorescently labeled particles had a diameter of approximately 100 nm and the larger fluorescently labeled ones were in the order of 1100 nm. The coating of the particles by PEGylation had no significant effect on the size. In addition non-modified 240-nm silica particles were tested. The crocidolite fibers used in this study were previously reported to have an average diameter of 180 nm (Nymark et al., 2014).



Sample	Hydrodynamic diameter measured by DLS (nm)	diameter measured by TEM (nm)
100 nm fluorescent	108 ± 18	100
1140 nm fluorescent	1100 ± 150	1140
100 nm pegylated	108 ± 18	100
1140 nm pegylated	1120 ± 150	1140
240 nm silica	120 ± 11	/

Figure 2. Characterization of silica-based MNP and PEG-functionalized silica-based MNP(A-D) showing TEM pictures of fluorescent silica particles (A) 100 nm and (B) 1140 nm, as well as PEG-functionalized fluorescent silica particles (C) 100 nm and (D) 1140 nm. The table resumes the diameters of the used nanoparticles measured by TEM and DLS.

4.3 Cellular toxicity assessment in iMeso-WT1, iMeso-NF3 and RN5 cells after exposure to five newly synthetized nano materials in vitro

Experiments were carried out using essentially the same parameters (doses, time points) as for the asbestos experiments. Based on previous reports that non-fibrous nanomaterials tend to show less cellular toxicity, the dose range was adjusted to 2 to 28 μg/cm². As a first observation all 5 materials were less toxic than asbestos fibers in all three cell lines tested (Fig. 3). Moreover there was no systematic difference in the toxicity profiles among the 3 cell lines. A small dose-dependent decrease in the cell viability was observed with all 5 nanomaterials and was most pronounced for the large Nano30 particles. Significant differences were only observed with the fluorescently labeled, non-PEGylated Nano31 and Nano 30; the larger particles Nano30 tended to be slightly more toxic than the smaller ones (Fig. 3). Of note, the toxicity almost disappeared when the particles were coated by PEG, i.e. both the smaller Nano34 and the larger Nano35 didn't affect growth/viability of all mesothelium-derived cells. The particles Nano90 of 240 nm diameter without any surface modifications didn't evoke any cytotoxic response in all cell lines at the doses tested.

4.4 iMeso-NF3-AsbR cells show a lasting increased resistance towards crocidolite-induced cytotoxicity compared to the parental iMeso-NF3 cells

iMeso-NF3 cells were 'chronically' exposed to 4 μg/cm² of crocidolite for 28 days, a dose causing rather significant toxicity already after 5 days (Fig. 1B). The cells that resisted this treatment were named iMeso-NF3-AsbR. A comparison of the growth characteristics of the initial iMeso-NF3 cells with the selected resistant iMeso-NF3-AsbR cells revealed that the asbestos-exposed cells proliferated faster (Fig. 4A). More importantly, when iMeso-NF3-AsbR cells were again exposed to crocidolite for 5 days at a dose range of 0.5 μg/cm² to 14 μg/cm², the viability compared to iMeso-NF3 cells was significantly increased (Fig. 4B), i.e. they were clearly more resistant to asbestos toxicity. Differences in cell viability and proliferation were already detected at a low-dose exposure of 0.5 μg/cm² and up to a dose of 2 μg/cm² iMeso-NF3-AsbR were as resistant as the RN5 mesothelioma cells. Also at higher doses iMeso-NF3-AsbR cells were more resistant than the parental cells and only slightly less resistant than RN5 tumor cells. Since the loss of one *Nf2* allele in iMeso-NF3 cells increased their sensitivity to asbestos toxicity (Fig. 1B), we investigated NF2 protein levels in all three cell lines in order to possibly detect a correlation between asbestos resistance and NF2 levels. The rather similar (normalized) NF2 protein levels in iMeso-NF3 and iMeso-NF3-AsbR cells (Fig. 2C) indicate that NF2 protein levels are likely neither directly involved in the faster proliferation (Fig. 4A) nor in the acquired increased asbestos resistance observed in iMeso-NF3-AsbR cells (Fig. 4B).

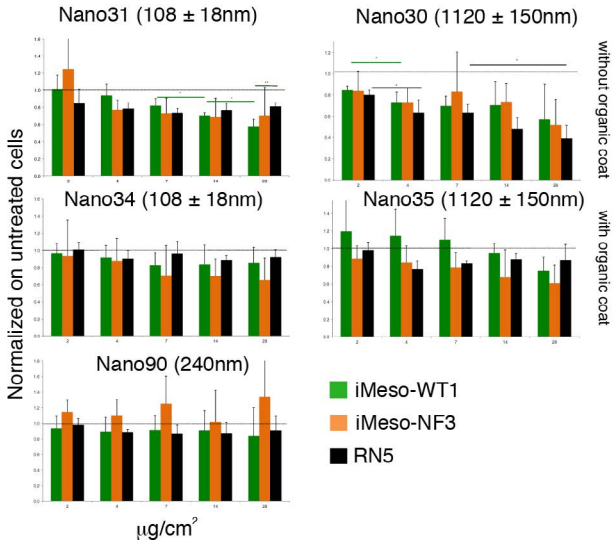


Figure 3. Dose-dependent cytotoxicity of silica-based nanoparticles in mesothelium-derived cells after 5 days of exposure. RN5 and iMeso cells were exposed to silica-based nanoparticles for 140h at densities ranging from 2 to 28 μg/cm². Nano30 and 31 are fluorescently labeled, but non-coated particles. In all cell lines, PEGylated silica nanoparticles were less cytotoxic than the "uncoated" ones. Nano90 are spherical non-modified silica particles showing a very weak effect on cell viability and proliferation. The lines with asterisk(s) above represent statistically significant differences between cell lines. The asterisks indicate the p-values: * = $p<0.05$, ** = $p<0.005$ and *** = $p<0.0005$, N=4.

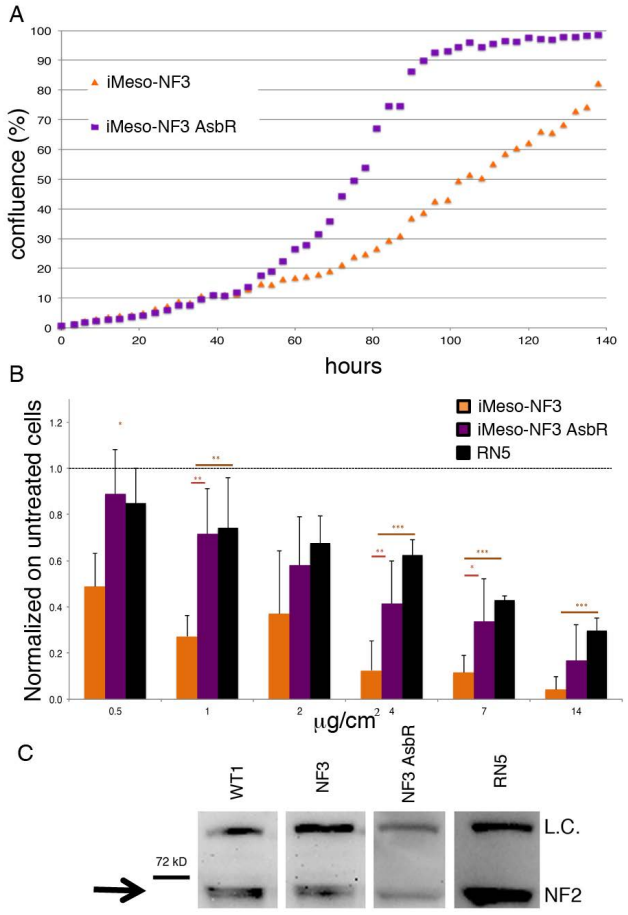


Figure 4. Real-time growth curves and MTT assays of RN5, iMeso-NF3 and iMeso–NF3-AsbR cells exposed to crocidolite for 140h. (A) iMeso-NF3-AsbR proliferated significantly faster than iMeso-NF3 cells. (B) iMeso-NF3-AsbR were significantly more resistant to crocidolite exposure than the parental iMeso-NF3: at low density exposure (up to 2 µg/cm^2), the crocidolite resistance was as high as in RN5 mesothelioma cells. The lines with asterisk(s) above represent the statistically significant differences. The asterisks indicate the p-values: * = p<0.05, ** = p<0.005 and *** = p<0.0005. N=3 independent experiments. (C) Western Blot analysis showing NF2 expression in samples from iMeso-WT1, iMeso-NF3, iMeso-NF3-AsbR and RN5. An unspecific biotinylated protein served as a loading control (l.c.;upper band).

4.5 Only RN5 mesothelioma cells form intraperitoneal tumors,while "chronically" exposed iMeso-NF3-AsbR cells do not

RN5 and iMeso-NF3-AsbR cells were injected intraperitoneally (i.p.) into WT C57Bl/6J mice and tumor formation was monitored. As soon as palpable tumors were detected (37 days after injection with RN5 cells), mice were sacrificed and tumors were analyzed at macroscopic and microscopic levels (Figs. 5A,B).RN5 cells were previously shown to be tumorigenic in subcutaneous xenograft experiments (Blum et al., 2015b), but here we demonstrated RN5's orthotopic tumor forming capacity. Since no palpable tumors were detected in mice injected with iMeso-NF3-AsbR cells, an upper time limit of 50 days post-injection was chosen, when mice were sacrificed and subjected to analyses (Fig. 5C, D). Mice injected with RN5 cells developed macroscopic i.p. tumors in congenic C57Bl/6J mice (Fig. 5A), generally observed as rather well delimited globular accumulations of tumor cells in the tunica serosa of the abdominal walls (Fig. 5A, inset), as well as on the surface of organs including the kidney (Fig. 5B). No signs of macroscopic tumors were observed in mice injected with iMeso-NF3AsbR(Fig. 5C); the tunica serosa covering the body cavity as well as the surface of organs including the spleen (Fig. 5D) appeared completely normal without any signs of serosa thickening or granuloma development. Thus, these results are in line with ones obtained with iMeso-NF3 cells that also failed to develop tumors in the s.c.tumor model (Blum et al., 2015b). Thus, the increased resistance of iMeso-NF3-AsbR cells towards acute asbestos toxicity is not sufficient to lead to a transformed phenotype or the time span (50 days) was too short to allow for the development of mesothelioma.

4.6 Lower spontaneous cell death rates of iMeso-NF3-AsbR cells are a likely cause for the increased proliferation in comparison to iMeso-NF3 cells

iMeso-NF3 cells transduced with cell cycle indicators (iMeso-NF3-CCI) were exposed as described above for 4 weeks to 4 µg/cm^2 of asbestos. The surviving "asbestos-resistant" cell population (iMeso-NF3-AsbR-CCI) was split into two groups; one was let to recover from asbestos treatment for 2 weeks and the other cell population was continually exposed to asbestos for another 2 weeks (iMeso-NF3-AsbR+2-CCI). The parental iMeso-NF3-CCI as well as the two asbestos-treated ones were then exposed to asbestos and cell viability was measured 5 days later (Figure 6A). iMeso-NF3 cells continuously exposed to asbestos were significantly more resistant than the parental iMeso-NF3 cells indicating that this cell population had acquired features transiently protecting

them from asbestos cytotoxicity. However this property disappeared when iMeso-NF3-AsbR cells were let to recover for two weeks from the asbestos exposure. Analyses of the cell cycle duration and the length of the G_0/G_1 and $S/G_2/M$ phases showed no significant differences between iMeso-NF3-AsbR and iMeso-NF3 cells (Figure 6B). Additionally, spontaneous cell death in the three cell populations was measured for 72 h after cell passaging (Figure 6C). Shortly after passaging, cell death (proportional to fluorescence intensity) was highest in all 3 cell lines, likely due to passaging stress and then decreased to reach a near steady-state approximately at 20 h post-passaging in all cell lines. In the period from 24 h to 72 h fluorescence levels in iMeso-NF3-AsbR cells-containing wells was clearly lower than in iMeso-NF3 and iMeso-NF3-AsbR2 cells demonstrating that spontaneous cell death rates were lower in continuously asbestos-exposed cells, a feature that is rapidly lost in cells let to recover from asbestos exposure (Figure 6C). In summary, growth differences between iMeso-NF3 and iMeso-NF3-AsbR are mostly due to decreased spontaneous cell death in the asbestos-resistant cell population. In addition the cell cycle analysis hint towards a slightly shorter $S/G_2/M$ phase in these cells (Figure 5B) that might partly contribute the increased growth phenotype considering its effect in an exponentially growing cell population.

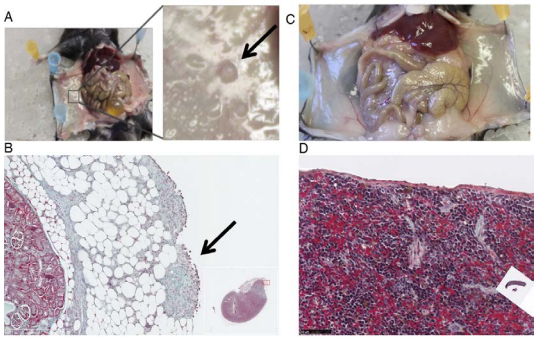


Figure 5. Testing of ***in vivo*** tumorigenicity of i.p.-injected RN5 and iMeso-NF3-AsbR cells in C57Bl/6J WT mice (A) Injected RN5 cells show strong tumorigenicity with *in situ* tumor formation on the parietal pleura after 37 days (arrow in the inset depicting a macroscopic tumor) and (B)Goldner staining showing tumor tissue located on the surface of the kidney (visceral pleura; arrow) and white adipose tissue as part of the tunica serosa. (C, D). In mice injected with iMeso-NF3-AsbR cells, no macroscopically detectable tumors were observed; a smooth parietal mesothelium and a normal tunica serosa covering the various organ surfaces were observed (C). On histological section, (...) no signs of iMeso-NF3-AsbR cell accumulation were observed. As an example the spleen covered with a single mesothelial cell layer (arrow) didn't show any signs of additional, adherent or abnormal cells (D).

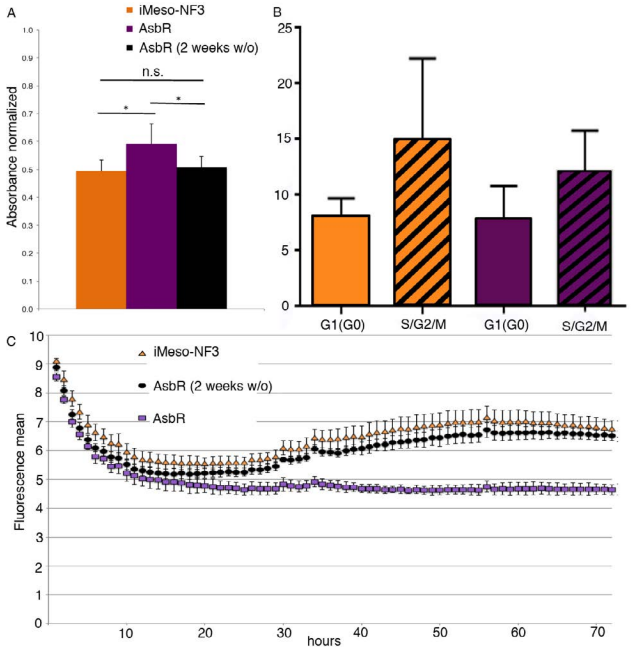


Figure 6. MTT assay after asbestos exposure for 120 h, Cell cycle analysis of parental and asbestos-resistant iMeso-NF3 cells and real-time cell death assay of iMeso-NF3, iMeso-NF3-AsbR and iMeso-NF3-AsbR+2 cells. (A) iMeso-NF3-AsbR cells additionally expressing cell cycle indicator were better protected against asbestos-induced cytotoxicity than iMeso-NF3 cells. Resistant cells grown for another 2 weeks in the absence of asbestos (iMeso-NF3-AsbR+2) lost their acquired resistance. (B) Cell cycle length evaluated by Fucci (fluorescent cell cycle indicators) was not significantly different in iMeso-NF3 and iMeso-NF3-AsbR cells. (C) Cell death was monitored for 72 h after cell passaging and showed a decrease in spontaneous cell death in iMeso-AsbR compared to parental iMeso-NF3. The asterisks indicate the p-values: * = $p<0.05$.

5. Discussion

Cell lines are essential model systems to test for nanotoxicity, especially mesothelial cells represent a very sensitive and biologically relevant model to test nanotoxicity and nanomaterial-induced tumorigenicity. To date, few studies on mesothelial cells concerning nanotoxicity have been performed. Here we investigated the acute effects of crocidolite on the growth of immortalized murine mesothelial cells iMeso-WT3 and iMeso-NF3, as well as on RN5 mouse mesothelioma cells. In our study we showed that lines of murine mesothelial cell origin are very sensitive towards crocidolite-induced cytotoxicity as well as to MNP, especially the cell line iMeso-NF3 was more than twice as sensitive the other cell lines we tested. They represent novel model systems of high biological

relevance, since asbestos exposure leads to tumor development and mesothelial cells belong to the most sensitive ones towards crocidolite-induced tumorigenesis. As reported in many studies, nanomaterials induce acute toxicity (Donaldson and Poland, 2009; Horváth et al., 2011; 2013; Magrez et al., 2009) and reproducibility is an important issue in the nanotoxicology field (Poland et al., 2014). Our results showed RN5 mesothelioma cells as well as the immortalized iMeso-NF3 and iMeso-WT1 cells to be reliable cell lines for testing acute nanomaterial toxicity. Their C57Bl/6J genetic background allows for *in vivo* experiments with this mouse strain, where many genetic models (e.g. knockout mice) have been developed. Thus, MNP toxicity may be assessed *in vivo* in mice with an intact immune system, where genes suspected to be implicated in tumorigenesis were deleted or mutated (e.g. putative tumor suppressor genes such as *Nf2* (Altomare, 2005), *Bap-1* (Napolitano et al., 2015)) or where proto-oncogenes were up-regulated or constitutively activated (Jongsma et al., 2008).

iMeso-NF3 cells showed higher susceptibility towards asbestos exposure compared to RN5 cells and hence non-transformed immortalized cells are excellent tools to study nanofiber toxicity *in vitro*. "Chronic crocidolite exposure", i.e. continuous exposure of mesothelial cells heterozygous for the tumor suppressor *Nf2* increased the resistance of the surviving cells to acute cytotoxicity; however the presumed changes in the resistant cells were insufficient for transformation evidenced by their incapacity to form tumors *in vivo*. A comparison of iMeso-NF3 and iMeso-NF3-AsbR cells might shed light on the mechanism leading to the increased resistance *in vitro*. Although iMeso-NF3 cells are monoclonal (i.e. derived from a single cell obtained by limited dilution (Blum et al., 2015b), unlike the situation in mesothelioma *in vivo* (Comertpay et al., 2014), the chronic crocidolite exposure resulted in a sub-population of mesothelial cells not only differing in crocidolite resistance, but also in proliferation rate and spontaneous cell death. Chronic tissue repair, inflammation and the microenvironment are considered as key factors contributing to asbestos-induced mesothelioma genesis (Hillegass et al., 2010; Murphy et al., 2013; Robinson and Lake, 2005; Stahel et al., 2009). We consider the immortalized mesothelial cells to be particularly helpful for investigating the early steps of tumor development, also *in vivo*.

The tumor initiating capacity of RN5 mesothelioma cells has been described before only in the subcutaneous heterotopic model (Blum et al., 2015b). Here we showed that RN5 cells injected in the peritoneal cavity results in orthotopic tumors in congenic C57Bl/6J mice. These mice are fully immuno-competent unlike in other non-congenic or even xenograft models that require either pharmacological immunosuppression of mice or the use of immunosuppressed strains (e.g. NOD-SCID gamma). The intraperitoneal localization represents the 'natural' environment of these tumor cells. We conclude that both immortalized mesothelial cells and mouse mesothelioma cells are excellent models to investigate different aspects of mesothelioma formation. With respect to nanotoxicity a-side-by-side comparison of the 2 models is expected to yield more information about the mechanisms leading to the putative hazardous health effects of MNP.

All mesothelium-derived cell lines proved to be robust models to investigate nanomaterial-induced acute cytotoxicity. RN5 mouse mesothelioma cells, as well as the immortalized mouse mesothelial cell lines iMeso-NF3 and iMeso-WT3, all on the common C57Bl/6J background, represent biological model systems of high relevance, since mesothelial cells are extremely sensitive towards asbestos and nanomaterial exposure. Moreover, RN5 and iMeso-NF3 are heterozygous for the tumor suppressor gene*Nf2*, a gene most often mutated in human MM. Side-by-side comparison revealed RN5 to be more resistant towards asbestos-induced cell death than iMeso-NF3; yet chronic asbestos treatment of iMeso-NF3 resulted in an increase in resistance that might be linked to early steps of carcinogenesis. In summary, mesothelium-derived cell models allow for an assessment of the hazardous effects of nanomaterials *in vitro* and possibly to dissect the mechanisms leading to MM formation *in vivo*.

5.1 Funding

The University of Fribourg, Switzerland, Swiss National Foundation (SNF grant 130680 to B.S.), SNF Sinergia grant CRSII3 147697/1, San Salvatore Foundation.

6. Acknowledgments

The authors want to thank Valérie Salicio, Simone Eichenberger, Marlène Sanchez and Martine Steinauer from the University of Fribourg, Switzerland for excellent technical assistance. The authors also want to thank Christoph Geers from Adolphe Merkle Institute, Fribourg for the TEM characterization of the silica particles.

7. Declaration of Interest

The authors declare no conflicts of interest.

8. References

1. Altomare, D.A., 2005. A Mouse Model Recapitulating Molecular Features of Human Mesothelioma. Cancer Research 65, 8090–8095. doi:10.1158/0008-5472.CAN-05-2312
2. Blum, W., Pecze, L., Felley-Bosco, E., Schwaller, B., 2015a. Overexpression or absence of calretinin in mouse primary mesothelial cells inversely affects proliferation and cell migration. Respiratory Research 1–16. doi:10.1186/s12931-015-0311-6
3. Blum, W., Pecze, L., Felley-Bosco, E., Worthmüller-Rodriguez, J., Wu, L., Vrugt, B., de Perrot, M., Schwaller, B., 2015b. Establishment of immortalized murine mesothelial cells and a novel mesothelioma cell line. In Vitro Cell DevBiol Anim. doi:10.1007/s11626-015-9885-z
4. Blum, W., Schwaller, B., 2013.Calretinin is essential for mesothelioma cell growth/survival in vitro: A potential new target for malignant mesothelioma therapy? Int. J. Cancer 133, 2077–2088. doi:10.1002/ijc.28218
5. Bocchetta, M., Di Resta, I., Powers, A., Fresco, R., Tosolini, A., Testa, J.R., Pass, H.I., Rizzo, P., Carbone, M., 2000. Human mesothelial cells are unusually susceptible to simian virus 40-mediated transformation and asbestos cocarcinogenicity. Proc. Natl. Acad. Sci. U.S.A. 97, 10214–10219.
6. Comertpay, S., Pastorino, S., Tanji, M., Mezzapelle, R., Strianese, O., Napolitano, A., Baumann, F., Weigel, T., Friedberg, J., Sugarbaker, P., Krausz, T., Wang, E., Powers, A., Gaudino, G., Kanodia, S., Pass, H.I., Parsons, B.L., Yang, H., Carbone, M., 2014. Evaluation of clonal origin of malignant mesothelioma. J Transl Med 12, 301–301. doi:10.1186/s12967-014-0301-3
7. Dechézelles, J.-F., Griffete, N., Dietsch, H., Scheffold, F., 2013. A General Method to Label Metal Oxide Particles with Fluorescent Dyes Using Aryldiazonium Salts. Part. Part. Syst. Charact. 30, 579–583.doi:10.1002/ppsc.201300014
8. Donaldson, K., Poland, C.A., 2012. Inhaled nanoparticles and lung cancer - what we can learn from conventional particle toxicology. Swiss Med Wkly. doi:10.4414/smw.2012.13547
9. Donaldson, K., Poland, C.A., 2009. Nanotoxicology: new insights into nanotubes. Nat Nanotechnol 4, 708–710. doi:10.1038/nnano.2009.327
10. Felley-Bosco, E., Stahel, R., 2014. Hippo/YAP pathway for targeted therapy. Transl Lung Cancer Res 3, 75–83. doi:10.3978/j.issn.2218-6751.2014.02.03
11. Graf, C., Gao, Q., Schütz, I., Noufele, C.N., Ruan, W., Posselt, U., Korotianskiy, E., Nordmeyer, D., Rancan, F., Hadam, S., Vogt, A., Lademann, J., Haucke, V., Rühl, E., 2012. Surface functionalization of silica nanoparticles supports colloidal stability in physiological media and facilitates internalization in cells. Langmuir 28, 7598–7613. doi:10.1021/la204913t
12. Henzi, T., Blum, W.-V., Pfefferli, M., Kawecki, T.J., Salicio, V., Schwaller, B., 2009. SV40-Induced Expression of Calretinin Protects Mesothelial Cells from Asbestos Cytotoxicity and May Be a Key Factor Contributing to Mesothelioma Pathogenesis. The American Journal of Pathology 174, 2324–2336. doi:10.2353/ajpath.2009.080352
13. Hillegass, J.M., Shukla, A., Lathrop, S.A., MacPherson, M.B., Beuschel, S.L., Butnor, K.J., Testa, J.R., Pass, H.I., Carbone, M., Steele, C., Mossman, B.T., 2010. Inflammation precedes the development of human malignant mesotheliomas in a SCID mouse xenograft model. Annals of the New York Academy of Sciences 1203, 7–14. doi:10.1111/j.1749-6632.2010.05554.x
14. Horváth, L., Magrez, A., Burghard, M., Kern, K., Forró, L., Schwaller, B., 2013. Evaluation of the toxicity of graphene derivatives on cells of the lung luminal surface. Carbon 64, 45–60. doi:10.1016/j.carbon.2013.07.005
15. Horváth, L., Magrez, A., Golberg, D., Zhi, C., Bando, Y., Smajda, R., Horváth, E., Forró, L., Schwaller, B., 2011. In VitroInvestigation of the Cellular Toxicity of Boron Nitride Nanotubes. ACS Nano 5, 3800–3810. doi:10.1021/nn200139h
16. Jongsma, J., van Montfort, E., Vooijs, M., Zevenhoven, J., Krimpenfort, P., van der Valk, M., van de Vijver, M., Berns, A., 2008. A Conditional Mouse Model for Malignant Mesothelioma. Cancer Cell 13, 261–271. doi:10.1016/j.ccr.2008.01.030
17. Magrez, A., Horváth, L., Smajda, R., Salicio, V., Pasquier, N., Forró, L., Schwaller, B., 2009. Cellular Toxicity of TiO 2-Based Nanofilaments. ACS Nano 3, 2274–2280. doi:10.1021/nn9002067
18. Mosmann, T., 1983. Rapid colorimetric assay for cellular growth and survival: application to proliferation and cytotoxicity assays. J. Immunol. Methods 65, 55–63.
19. Murphy, F.A., Poland, C.A., Duffin, R., Donaldson, K., 2013.Length-dependent pleural inflammation and parietal pleural responses after deposition of carbon nanotubes in the pulmonary airspaces of mice.Nanotoxicology 7, 1157–1167. doi:10.3109/17435390.2012.713527
20. Mutsaers, S.E., 2004. The mesothelial cell. The International Journal of Biochemistry & Cell Biology 36, 9–16. doi:10.1016/S1357-2725(03)00242-5
21. Napolitano, A., Pellegrini, L., Dey, A., Larson, D., Tanji, M., Flores, E.G., Kendrick, B., Lapid, D., Powers, A., Kanodia, S., Pastorino, S., Pass, H.I., Dixit, V., Yang, H., Carbone, M., 2015. Minimal asbestos exposure in germline 1–7. doi:10.1038/onc.2015.243
22. Nymark, P., Jensen, K.A., Suhonen, S., Kembouche, Y., Vippola, M., Kleinjans, J., Catalan, J., Norppa, H., van Delft, J., Briede, J.J., 2014. Free radical scavenging and formation by multi-walled carbon nanotubes in cell free conditions and in human bronchial epithelial cells. Part FibreToxicol 11, –4. doi:10.1186/1743-8977-11-4

23. Pecze, L., Schwaller, B., 2015. Characterization and modeling of Ca(2+) oscillations in mouse primary mesothelial cells. Biochim. Biophys. Acta 1854, 632–645. doi:10.1016/j.bbamcr.2014.12.025
24. Poland, C.A., Miller, M.R., Duffin, R., Cassee, F., 2014. The elephant in the room: reproducibility in toxicology. Part FibreToxicol 11, 42.doi:10.1186/s12989-014-0042-8
25. Robinson, B.W.S., Lake, R.A., 2005. Advances in malignant mesothelioma. N. Engl. J. Med. 353, 1591–1603. doi:10.1056/NEJMra050152
26. Stahel, R.A., Felley-Bosco, E., Opitz, I., Weder, W., 2009. Malignant pleural mesothelioma.Future Oncology 5, 391–402.doi:10.2217/fon.09.7
27. Stark, W.J., Stoessel, P.R., Wohlleben, W., Hafner, A., 2015. ChemSoc Rev. ChemSoc Rev 1–13. doi:10.1039/C4CS00362D
28. Szabolcsi, V., Celio, M.R., 2015. De novo expression of parvalbumin in ependymal cells in response to brain injury promotes ependymal remodeling and wound repair. Glia 63, 567–594. doi:10.1002/glia.22768
29. Thurneysen, C., Opitz, I., Kurtz, S., Weder, W., Stahel, R.A., Felley-Bosco, E., 2009. Functional inactivation of NF2/merlin in human mesothelioma. Lung Cancer 64, 140–147. doi:10.1016/j.lungcan.2008.08.014
30. Verhaegh, N., Blaaderen, A., 1994. Dispersions of rhodamine-labeled silica spheres: synthesis, characterization, and fluorescence confocal scanning laser microscopy. Langmuir.